Technical Physics, 2023, Vol. 68, No. 3

13

Record thick $\kappa(\varepsilon)$-Ga_2O_3 epitaxial layers grown on GaN/c-sapphire

© V.I. Nikolaev,[1,3] A.Ya. Polyakov,[2] S.I. Stepanov,[1,3] A.I. Pechnikov,[1] V.V. Nikolaev,[3] E.B. Yakimov,[4] M.P. Scheglov,[1] A.V. Chikiryaka,[1] L.I. Guzilova,[1] R.B. Timashov,[1] S.V. Shapenkov,[1] P.N. Butenko[1]

[1] Ioffe Institute, St. Petersburg, Russia
[2] National University of Science and Technology MISiS, Moscow, Russia
[3] Perfect Crystals LLC, Saint-Petersburg, Russia
[4] Institute of Microelectronics Technology, Chernogolovka, Moscow reg., Russia
e-mail: luba-guzilova@yandex.ru

Received October 4, 2022
Revised December 30, 2022
Accepted January 10, 2022

Record thick (up to 100 μm) epitaxial layers of a prospective metastable semiconductor Ga_2O_3 were grown by HVPE (Halide Vapor Phase Epitaxy) on GaN buffer layers on c-sapphire substrates. The X-ray diffraction pattern of the layers show that the structure of the layer is a pure $\kappa(\varepsilon)$-Ga_2O_3 without any other phases. At the same time, the organization of a domain structure was observed, which manifests itself in the form of pseudohexagonal prisms that retain the orientation of the gallium nitride sublayer. Schottky diodes with nickel contacts were fabricated and the electrical and photoelectric properties of the layers were studied. Capacitance-voltage ($C-V$) and frequency-capacitance ($C-f$) dependencies were studied, photocurrent and photocapacitance spectra were measured.

Keywords: Gallium oxide, HVPE, epitaxial layers, sapphire substrates.

DOI: 10.21883/TP.2023.03.55813.231-22

Introduction

Gallium oxide and its solid solutions are currently of great interest due to their wide band gaps near 5 eV, the availability of controlled n-type doping, sufficiently high electron mobilities and saturation rates, and high photosensitivity in the far UV region of the spectrum. This set of properties makes epitaxial layers of this material promising for use in the structures of high-power and high-voltage diodes, solar-blind ultraviolet photodetectors [1–3]. It is worth noting that gallium oxide forms several polymorphic modifications (α-, β-, γ-, δ-, $\kappa(\varepsilon)$-phases), of which only β-Ga_2O_3 with a monoclinic crystal lattice is thermodynamically stable up to its melting at $T \sim 1800°C$. This polymorph has attracted researchers to a greater extent. However, metastable polymorphs [4] have a number of advantages over β-Ga_2O_3, and recently come to the forefront of semiconductor physics [5–8]. Note that $\kappa(\varepsilon)$-Ga_2O_3 is the only polar crystal among the polymorphs, exhibiting spontaneous polarization that is about an order of magnitude higher than that in semiconductor nitrides [9,10]. This opens up the possibilities of so-called „polarization" doping, enabling the creation of a very high density of two-dimensional electron gas (2DEG) for implementation in high electron mobility transistors (HEMTs), which are expected to be better than existing high-power AlGaN/GaN based HEMTs [8]. Unfortunately, until now, the potential of $\kappa(\varepsilon)$-Ga_2O_3 has not been fully realized due to the low crystalline quality of the grown layers. $\kappa(\varepsilon)$-Ga_2O_3 tends to form 120° domains, presumably with a high density of dislocations between them, which greatly hinders in-plane conductivity in these films [11]. A significant progress has been achieved here through the use of ELOG (Epitaxial Lateral Overgrowth) technology. Recently, $\kappa(\varepsilon)$-Ga_2O_3 epitaxial films with strongly suppressed formation of rotational domains were obtained by this method [12]. We assume that some natural improvement in the layer quality is possible with an increasing thickness and moving away from the substrate due to the wedging out of defects, similar to what is observed in other wide-gap semiconductor crystals grown by the HVPE method [13].

There is still very little information about the spectra of electronic states in $\kappa(\varepsilon)$-Ga_2O_3. Below we inform about such studies carried out for Schottky diodes with a Ni-contact deposited on $\kappa(\varepsilon)$-Ga_2O_3 thick films grown by the HVPE method on GaN buffer layers on c-sapphire.

1. Experiment procedure

$\kappa(\varepsilon)$-Ga_2O_3 films were deposited in a horizontal HVPE quartz reactor with hot walls. Patterned c-plane sapphire wafers (PSS) with a preliminarily deposited buffer layer of gallium nitride GaN were used as substrates. The GaN layer thickness was 3–4 μm; in this case complete overgrowth of the relief irregularities of the patterned (PSS) was achieved resulting in the formation of a planar GaN layer. For $\kappa(\varepsilon)$-Ga_2O_3 deposition gaseous oxygen (O_2) and gallium chloride (GaCl) were used as the oxygen and gallium sources. GaCl vapor was produced in the reactor by flowing gaseous hydrogen chloride (HCl, 99.999%) above a boat with metallic gallium (Ga, 99.9999%). The HCl flow rate through the Ga source and the oxygen flow rate were 100 and 300 sccm, respectively. High-purity argon

(Ar) served as the carrier gas. Ga_2O_3 films were deposited at a temperature of 570°C under atmospheric pressure. The deposition rate was $3-4\,\mu$m/h. The obtained samples had a thickness ranging from 20 to $100\,\mu$m.

The crystal structure and crystal quality of Ga_2O_3 films were monitored using a Dron-6 X-ray diffractometer, in a two- and three-crystal scheme using $CuK_{\alpha 1}$ radiation ($\lambda = 1.5405$ Å). The thickness of $\kappa(\varepsilon)$-Ga_2O_3 films was determined using several methods: optical and scanning electron microscopy and (or) consistent weighing of samples using a precision balanc OHAUS EX324/AD before and after epitaxy.

The surface morphology of the grown films was analyzed in detail through observation on a Phenom PRO X scanning electron microscope (SEM) in the secondary electron (SE) mode.

Microcathodoluminescence (MCL) of the samples was performed on MonoCL-3 system (UK) at room temperature.

To characterize the electrical and photoelectric properties, semitransparent nickel Schottky contacts with a thickness of 20 nm and a diameter of 1.2 mm were used. These contacts were deposited by electron-beam evaporation through a shadow mask. Ohmic contacts were formed by electron-beam deposition of Ti/Au (20 nm/80 nm) through a shadow mask. The procedure for contact fabrication is described in [14,15].

For samples with deposited Schottky contacts and ohmic measurements of current-voltage $I-V$, capacitance-frequency $(C-f)$, capacitance-voltage $(C-V)$ were carried out in the dark conditions and under monochromatic illumination with a set of powerful light-emitting diodes (LEDs) with peak wavelength ranging from 365 to 950 nm and output optical power up to 250 mW/cm^2. For excitation above the band gap in these measurements, three LEDs grouped in parallel with a wavelength of 259 nm and a total output power close to 1.2 mW/cm^2 were used.

2. Experimental results and discussion

X-ray diffraction of the obtained thick $\kappa(\varepsilon)$-Ga_2O_3 layers shows that the layers are single-phase, they do not contain inclusions of other polymorphs, and they are oriented in the [001] direction. The X-ray diffraction pattern (Fig. 1) contains only strong even reflections from the (001) plane ranging from the 2nd to the 10th orders and weaker odd and similar of the 5th, 7th, and 9th orders. The full width at half maximum (FWHM) of the X-ray rocking curve (ω-scan) for 006 reflection of the 100-micron layer was about 1 deg.

Fig. 2 shows the surface morphology and cross-sectional image of the grown layer from which the thickness of $86\,\mu$m was determined. On a relatively smooth surface, hexagons of a regular shape, and similar size, are observed, they have a clear crystal-lattice orientation with respect to the substrate. Similar hexagonal figures were observed earlier during $\kappa(\varepsilon)$-Ga_2O_3 growth on other substrates [16]. Such

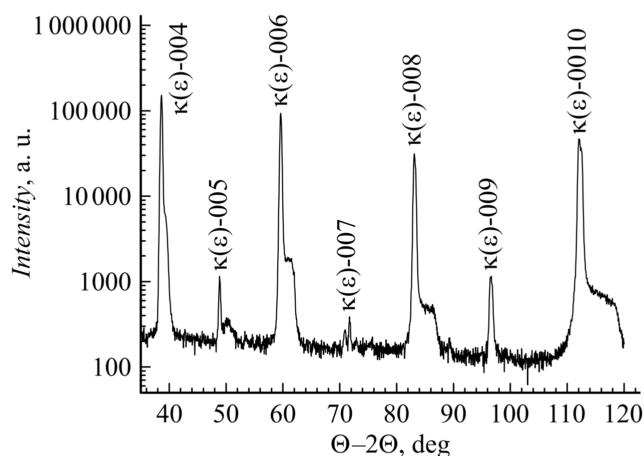

Figure 1. X-ray diffraction pattern of the $\kappa(\varepsilon)$-Ga_2O_3 film grown on a GaN/sapphire heatplate; five strong consecutive reflections: 002, 004, 006, 008, 0010 from the (001) plane $\kappa(\varepsilon)$-Ga_2O_3, odd reflections 005, 007 and 009 from the same plane.

formations are characteristic only for this polymorph, as they are not observed in the case of α- and β-Ga_2O_3 HVPE layers they are not observed. The hexagonal shape of the overgrowths, which gives the impression of a hexagonal structure of the polymorph, is actually associated with the formation of 120° rotating domains, rather than with the hexagonal symmetry of the crystal structure [12,17]. As previously shown in [12], the improvement of structural quality of the layer is can be achieved by additional technological methods, such as, ELOG technology, which can eliminate the formation of a polydomain structure.

The MCL spectrum of a $20\,\mu$m $\kappa(\varepsilon)$-Ga_2O_3 film obtained by HVPE is shown in Fig. 3. Its profile is similar to that observed earlier on $\kappa(\varepsilon)$-Ga_2O_3 layer obtained by metal organic chemical vapor deposition method (MOCVD) [1,18], and on $\kappa(\varepsilon)$-Ga_2O_3 thin films from HVPE processes [19]. The MCL band ranging from 2 to 3.5 eV in our measurements can be reasonably approximated by four Gaussian curves with peaks at 2.59, 2.66, 2.86, and 3.12 eV. The peak energies are close to those reported in [1,19], but slightly differ from [20].

I–Vs of Schottky diodes with nickel contacts, fabricated on grown $\kappa(\varepsilon)$-Ga_2O_3 films, are presented for three temperatures (130, 296 and 420 K) in Fig. 4. In all cases, the rectification factor was quite high, and the leakage current was relatively low. However, the ideality factor noticeably deviated from 1 (2.6 at room temperature and 1.8 at 420 K), and at low forward voltages the current was determined by leakage. Measurements of the temperature dependence of the forward current at 2 V (when this dependence is determined by the series resistance of the diode) yielded a value of 0.3 eV. The diode showed a rather high photosensitivity, especially when excited by photons with energies above the band gap, which is technically implemented using a 259 nm LED (Fig. 5, *a*).

Capacitance vs. frequency $C-f$ measurements at for 130, 296 and 420 K, measured at 0 V, are shown in Fig. 6, *a*. It

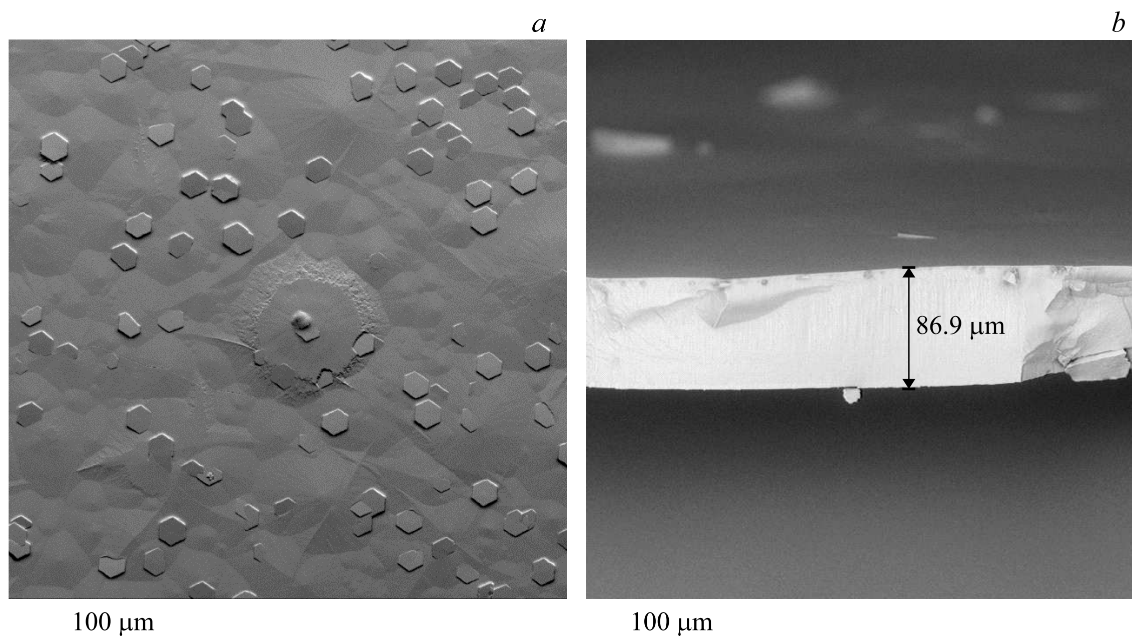

Figure 2. SEM images of the surface of $\kappa(\varepsilon)$-Ga_2O_3 layer, 86 μm thick: *a* — plan-view of the (001) surface and *b* — cross section plate splintering.

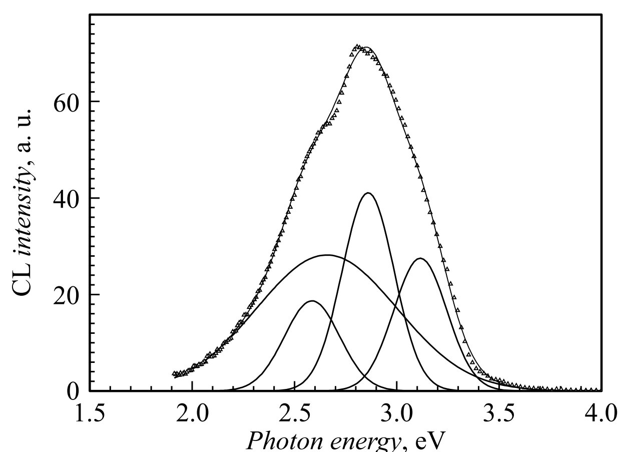

Figure 3. An example of the approximation of the micro-cathodoluminescence spectrum of the $\kappa(\varepsilon)$-Ga_2O_3 layer at room temperature with beam energy of 10 keV and beam current of 0.1 nA.

can be seen that the frequency dependence of the capacitance at room temperature shows a noticeable increase in capacitance at low frequencies. At higher temperature, this region turns into a step, indicating the predominance, along with shallow donors responsible for the high-frequency capacitance at room and low temperatures, of deeper centers, whose exchange rate with the conduction band carriers becomes sufficiently fast. Measurement of the concentration distribution profile of these centers at a high temperature at a frequency of 20 Hz shows that they are concentrated in a thin layer near the surface with a thickness of about 0.1 μm and have a very high concentration of $1.2 \cdot 10^{17}\,cm^{-3}$. Measurements of the dependence of capacitance and conductivity at different frequencies on temperature show that the depth of these centers is 0.7 eV. At room temperature, when measuring the dependence of the capacitance on voltage at frequency corresponding to the „plateau“ in the frequency dependence of capacitance (100 kHz), it was found that the upper part of the film 1.8 μm thick is completely depleted of carriers. In a deeper region the concentration of donors responding to the test voltage with frequency of 100 kHz is $10^{16}\,cm^{-3}$, but the cutoff voltage in the dependence

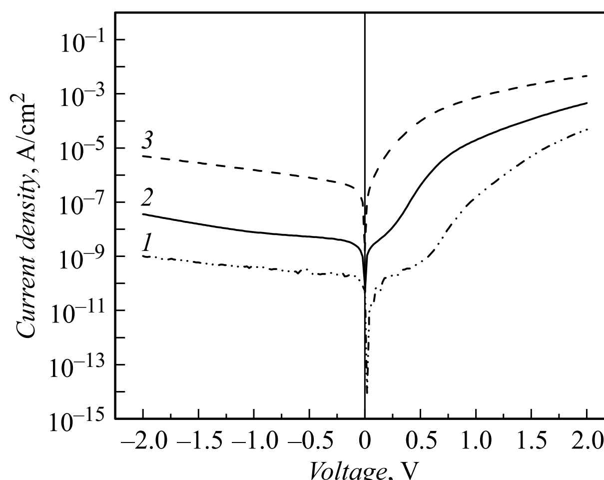

Figure 4. I–V of Schottky diode with Ni-contact and $\kappa(\varepsilon)$-Ga_2O_3-layer, measured for three temperatures, K: 130 (*1*), 297 (*2*), 420 (*3*).

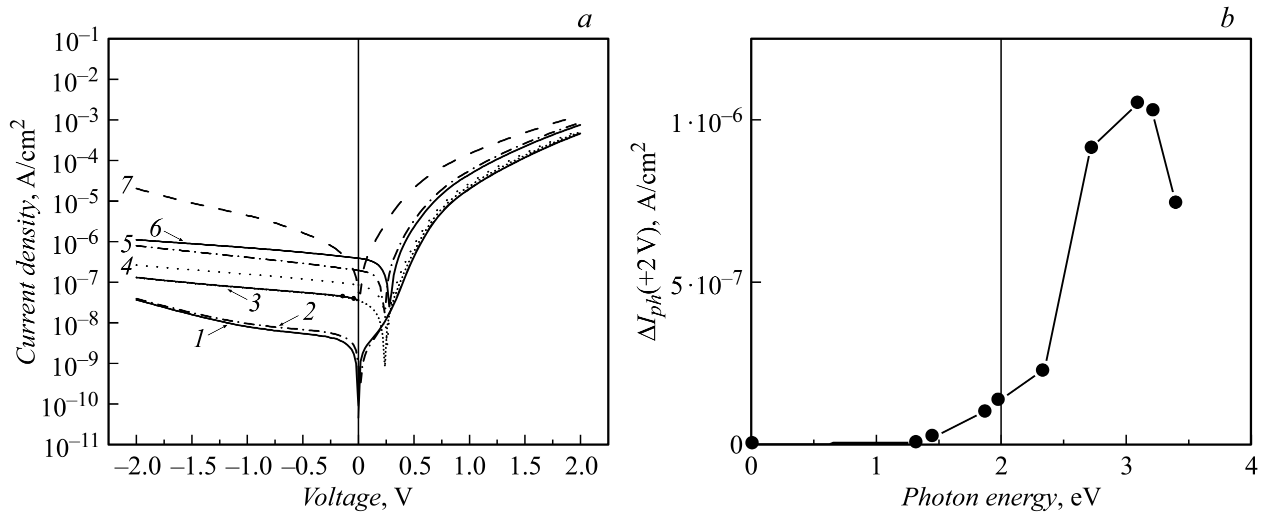

Figure 5. a — I–V of $\kappa(\varepsilon)$-Ga_2O_3 layer $20\,\mu$m thick in darkness (*1*) and under illumination of $250\,mW/cm^2$ by LEDs with different wavelengths, nm: 940 (*2*), 660 (*3*), 530 (*4*), 400 (*5*), 365 (*6*), 259 (*7*); b — spectral dependence of the forward current at 2 V.

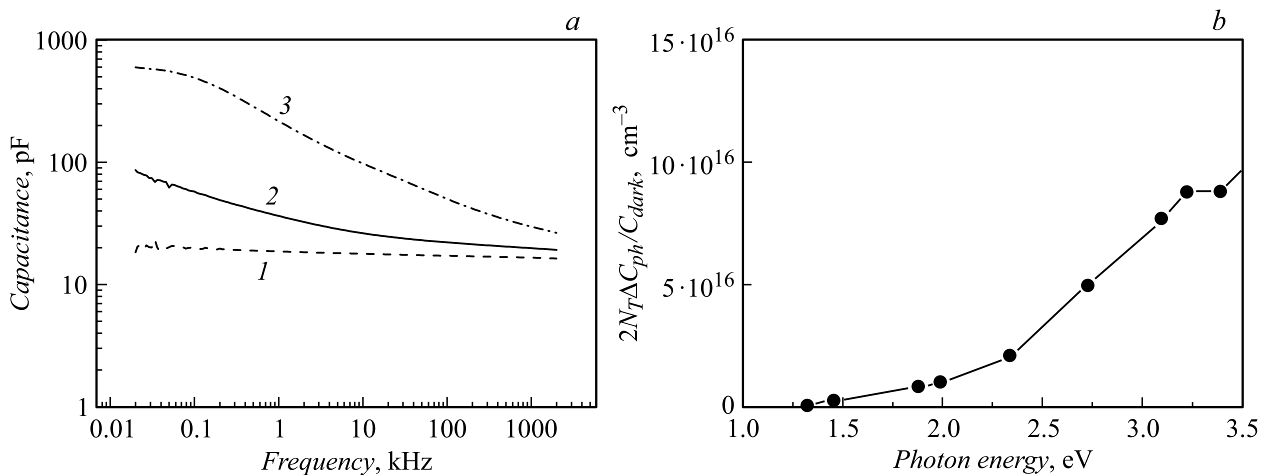

Figure 6. a — $C-f$ dependences of the $\kappa(\varepsilon)$-Ga_2O_3 layer at temperatures, K: 130 (*1*), 297 (*2*), 420 (*3*) without illumination and displacement (at 0 V); b — spectrum $2N_T\Delta C_{ph}/C_{dark}$ for $T = 420$ K and $f = 20$ Hz.

of $1/C^2$ on the voltage is very large. This is due to a large voltage drop in the near-surface region with deeper donors, the depth of which can be estimated from the temperature dependence of the forward current as 0.3 eV (see above). It is evident from the above analysis that the near-surface region of the film $0.1\,\mu$m thick is enriched with deep centers at a level of 0.7 eV from the edge of the conduction band, while the region $1.8\,\mu$m thick is enriched with centers with depth of about $1.8\,\mu$m. The lication of the Fermi level in different parts of the film, is determined by the balance between the concentration of donor centers at 0.3, and 0.7 eV and the concentration of deep acceptors. The type and concentration of the latter can be determined from the photocapacitance spectra ΔC_{ph}. Fig. 6, b shows $2N_T\Delta C_{ph}/C_{dark}$ spectrum obtained for 0 V and 20 Hz (where N_T is the total concentration of traps at 0.7 eV, which determines the space charge width for the low-frequency and $C-V$ profile C_{dark} — dark capacitance at 0 V and 20 Hz). This value makes it possible to approximately determine the concentration of deep acceptors compensating the conductivity in the near-surface region $0.1\,\mu$m thick [20]. The spectrum reveals two optical thresholds at around 1.35 and 2.3 eV, similar to those observed in the photocurrent spectra at forward current (Fig. 5, b). The concentration of these compensating acceptors is about $10^{16}\,cm^{-3}$ for centers with an energy 1.35 eV and $7.8 \cdot 10^{16}\,cm^{-3}$ for centers with an optical ionization threshold of about 2.3 eV.

The photocapacitance spectra at a frequency of 100 kHz showed the same optical ionization thresholds as at 20 Hz, However the concentrations of the corresponding deep traps calculated using a donor concentration of around $10^{16}\,cm^{-3}$ determined from voltage-capacitance measurements at 100 kHz were close to $4 \cdot 10^{14}\,cm^{-3}$ for centers

1.35 eV and 1015 cm^{-3} — for centers 2.3 eV, i.e. the concentrations of compensating acceptors increased by approximately two orders of magnitude as the surface was approached.

Conclusion

Super thick $\kappa(\varepsilon)$-Ga_2O_3 layers, with thickness up to 100 μm, were obtained by the HVPE. The proposed method allows for the attainment of even greater thickness, making it possible to consider the layer as a quasi-bulk substrate for subsequent homoepitaxy. X-ray diffraction analysis of the layers showed the absence of other polymorphic phases, except for $\kappa(\varepsilon)$-Ga_2O_3. The FWHM value determined from the rocking curve indicates a satisfactory crystalline quality even for such thick epitaxial layers. In a sense, the proposed method for fabricating quasi-bulk $\kappa(\varepsilon)$-Ga_2O_3 layers can be considered as an alternative to the liquid-phase bulk growth of β-Ga_2O_3, since $\kappa(\varepsilon)$-Ga_2O_3 is a sufficiently thermally stable phase. The transition from $\kappa(\varepsilon)$-Ga_2O_3 to β-Ga_2O_3 can occur only at $T > 800°C$. From both technological and commercial perspectives, this method of obtaining the substrate is more preferable than the melt growth of the β-polymorph, which has proven to be quite challenging due to gallium oxide dissociation at high temperatures. In terms of electrical and photoelectric properties, the obtained layers are close to the thin layers obtained earlier [4]. The electronic properties of the layer, as we found, do not strongly depend on its thickness. Summary, $\kappa(\varepsilon)$-Ga_2O_3 in its functional properties is not inferior to β-Ga_2O_3, and due to its polar properties and compatibility with GaN it has great prospects.

Funding

V.I. Nikolaev, A.Ya. Polyakov, S.I. Stepanov, A.I. Pechnikov, L.I. Guzilova express their gratitude to the Russian Science Foundation for supporting the study under the grant № 19-19-00409.

Conflict of interest

The authors declare that they have no conflict of interest.

References

[1] S.J. Pearton, F. Ren, M. Tadjer, J. Kim. J. Appl. Phys., **124** (22), 220901 (2018). DOI: 10.1063/1.5062841
[2] M. Higashiwaki, S. Fujita. *Gallium Oxide: Materials Properties, Crystal Growth, and Devices* (Springer, 2020)
[3] J. Xu, W. Zheng, F. Huang. J. Mater. Chem. C, **7** (29), 8753 (2019). DOI: 10.1039/C9TC02055A
[4] A. Polyakov, V. Nikolaev, A. Pechnikov, S. Stepanov, E. Yakimov, M. Scheglov, I.V. Shchemerov, A. Vasilev, A. Kochkova, A. Chernykh, A.V. Chikiryaka, S.J. Pearton. APL Mater., **10** (6), 061102 (2022). DOI: 10.1063/5.0091653
[5] M.B. Maccioni, V. Fiorentini. Appl. Phys. Express, **9** (4), 041102 (2016). DOI: 10.7567/APEX.9.041102
[6] E. Ahmadi, Y. Oshima. J. Appl. Phys., **126** (16), 160901 (2019). DOI: 10.1063/1.5123213
[7] A.Y. Polyakov, V.I. Nikolaev, E.B. Yakimov, F. Ren, S.J. Pearton, J. Kim. J. Vac. Sci. Technol. A, **40** (2), 020804 (2022). DOI: 10.1116/6.0001701
[8] M. Biswas, H. Nishinaka. APL Mater., **10**, 060701 (2022). DOI: 10.1063/5.0085360
[9] J. Kim, D. Tahara, Y. Miura, B.G. Kim. Appl. Phys. Express, **11** (6), 061101 (2018). DOI: 10.7567/APEX.11.061101
[10] S.Yu. Davydov. Physics Solid State, **51** (6), 1231 (2009). DOI: 10.1134/S1063783409060249
[11] M. Kneiß, D. Splith, P. Schlupp, A. Hassa, H. von Wenckstern, M. Lorenz, M. Grundmann. J. Appl. Phys, **130**, 084502 (2021). DOI: 10.1063/5.0056630
[12] Y. Oshima, K. Kawara, T. Oshima, T. Shinohe. Jpn. J. Appl. Phys., **59** (11), 115501 (2020). DOI: 10.35848/1347-4065/abbc57
[13] X.H. Wu, L.M. Brown, D. Kapolnek, S. Keller, B. Keller, S.P. DenBaars, J.S. Speck. J. Appl. Phys., **80** (6), 3228 (1996). DOI: 10.1063/1.363264
[14] A.Y. Polyakov, V.I. Nikolaev, S.I. Stepanov, A.I. Pechnikov, E.B. Yakimov, N.B. Smirnov, I.V. Shchemerov, A.A. Vasilev, A.I. Kochkova, A.V. Chernykh, S.J. Pearton. ECS J. Solid State Sci. Technol., **9**, 045003 (2020). DOI: 10.1149/2162-8777/ab89bb
[15] A.Y. Polyakov, N.B. Smirnov, I.V. Shchemerov, E.B. Yakimov, V.I. Nikolaev, S.I. Stepanov, A.I. Pechnikov, A.V. Chernykh, K.D. Shcherbachev, A.S. Shikoh, A. Kochkova, A.A. Vasilev, S.J. Pearton. APL Mater., **7** (5), 051103 (2019). DOI: 10.1063/1.5094787
[16] V.I. Nikolaev, S.I. Stepanov, A.I. Pechnikov, S.V. Shapenkov, M.P. Scheglov, A.V. Chikiryaka, O.F. Vyvenko. ECS J. Solid State Sci. Technol., **9** (4), 045014 (2020). DOI: 10.1149/2162-8777/ab8b4c
[17] I. Cora, F. Mezzadri, F. Boschi, M. Bosi, M. Čaplovičová, G. Calestani, I. Dódony, B. Pécz, R. Fornari. Cryst. Eng. Comm., **19**, 1509 (2017). DOI: 10.1039/C7CE00123A
[18] V. Montedoro, A. Torres, S. Dadgostar, J. Jimenez, M. Bosi, A. Parisini, R. Fornari. Mater. Sci. Eng. B, **264**, 114918 (2021). DOI: 10.1016/j.mseb.2020.114918
[19] S. Shapenkov, O. Vyvenko, V. Nikolaev, S. Stepanov, A. Pechnikov, M. Scheglov, G. Varygin. Phys. Status Solidi B, **259** (2), 2100331 (2021). DOI: 10.1002/pssb.202100331
[20] J.V. Li, G. Ferrari. *Capacitance Spectroscopy of Semiconductors* (Jenny Stanford Publishing, 2018)

Translated by I.Mazurov